

Is the Hénon attractor chaotic?

Zbigniew Galias and Warwick Tucker

Citation: *Chaos: An Interdisciplinary Journal of Nonlinear Science* **25**, 033102 (2015); doi: 10.1063/1.4913945

View online: <http://dx.doi.org/10.1063/1.4913945>

View Table of Contents: <http://scitation.aip.org/content/aip/journal/chaos/25/3?ver=pdfcov>

Published by the [AIP Publishing](#)

Articles you may be interested in

[Detecting variation in chaotic attractors](#)

Chaos **21**, 023128 (2011); 10.1063/1.3602221

[A lot of strange attractors: Chaotic or not?](#)

Chaos **18**, 023127 (2008); 10.1063/1.2937016

[Chaotic itinerancy generated by coupling of Milnor attractors](#)

Chaos **13**, 937 (2003); 10.1063/1.1599131

[Fluctuational Escape from Chaotic Attractors](#)

AIP Conf. Proc. **665**, 435 (2003); 10.1063/1.1584918

[Chaotic pendulum: The complete attractor](#)

Am. J. Phys. **71**, 250 (2003); 10.1119/1.1526465



Is the Hénon attractor chaotic?

Zbigniew Galias^{1,a)} and Warwick Tucker^{2,b)}

¹Department of Electrical Engineering, AGH University of Science and Technology, al. Mickiewicza 30, 30-059 Kraków, Poland

²Department of Mathematics, Uppsala University, Box 480, 751 06 Uppsala, Sweden

(Received 11 January 2015; accepted 17 February 2015; published online 5 March 2015)

By performing a systematic study of the Hénon map, we find low-period sinks for parameter values extremely close to the classical ones. This raises the question whether or not the well-known Hénon attractor—the attractor of the Hénon map existing for the classical parameter values—is a strange attractor, or simply a stable periodic orbit. Using results from our study, we conclude that even if the latter were true, it would be practically impossible to establish this by computing trajectories of the map. © 2015 AIP Publishing LLC. [<http://dx.doi.org/10.1063/1.4913945>]

Numerical studies suggest that the well-known Hénon attractor \mathcal{A} —the attractor of the Hénon map existing for the classical parameter values—is invariant, trajectories within \mathcal{A} display sensitive dependence on initial conditions, and almost all trajectories within \mathcal{A} form a dense subset of \mathcal{A} . Yet, it is important to remember that this is not a mathematically proven fact. An alternative possibility is that \mathcal{A} is a stable periodic orbit, attracting trajectories for almost all initial conditions. If this is the case, and the immediate basin of attraction of \mathcal{A} is very small, then the sink is numerically unstable unless the computations are carried out with sufficiently high precision. In this paper, we locate periodic windows extremely close to the classical parameter values. From our analysis, it follows that even when the computations are done with sufficient precision, we may need an extremely large number of iterations to observe a sink starting from random initial conditions. The conclusion is that most numerical studies do not display anything but transient behaviour; the true nature of the long-term dynamics of the Hénon map cannot be revealed by studying finite portions of trajectories.

I. INTRODUCTION

The Hénon map¹ is a two-parameter map of the plane defined by $h(x,y) = (1 + y - ax^2, bx)$. In Ref. 1, the map h is numerically studied with parameter values $(a,b) = (1.4, 0.3)$, and it is claimed that in this case, “depending on the initial point, the sequence of points obtained by iteration of the mapping either diverges to infinity or tends to a strange attractor.” In the following, we will refer to $(a^*, b^*) = (1.4, 0.3)$ as the *classical parameter values*, and we will call the attractor existing for classical parameter values the *Hénon attractor*. In spite of extensive study, the long-term dynamics of the Hénon map for the classical parameter values remains unknown. In this work, via numerical study, we attempt to answer the question whether the Hénon attractor is strange/chaotic as Hénon suggested or not.

^{a)}Electronic mail: galias@agh.edu.pl.

^{b)}Electronic mail: warwick@math.uu.se.

When $b = 0$, the Hénon map reduces to the quadratic map $f(x) = 1 - ax^2$. The set \mathcal{S}^- of parameter values for which the unique attracting set is a periodic sink is open and dense. On the other hand, the set \mathcal{S}^+ of parameter values with chaotic dynamics is a Cantor set with positive Lebesgue measure.² For the quadratic map, these two sets are disjoint, i.e., for each a , there exist at most one attractor, and their union $\mathcal{S}^+ \cup \mathcal{S}^-$ has full one-dimensional measure in the parameter space for a . When $b > 0$ is sufficiently small, the set of parameter values a with chaotic dynamics is also a Cantor set with positive Lebesgue measure.³

Numerical studies indicate that the situation of the quadratic map partially carries over to that of the Hénon map for macroscopic values of b . The general belief is that the set of parameter values with chaotic behavior still has positive measure, and that the set of parameter values with stable periodic behavior remains open and dense. But, there are also striking differences: it appears that the two sets \mathcal{S}^- and \mathcal{S}^+ may have non-empty intersection; there are parameters for which a strange attractor coexists with one or more sinks. If these hypotheses are true, it seems very unlikely that we will ever be able to prove that there exists a chaotic attractor for a specific point in the parameter space; an arbitrarily small perturbation may change the strange attractor into a sink. On the other hand, proving the existence of a sink is—in principle—not hard. Therefore, if the attractor is a sink, we may be able to establish this fact.

In this work, we propose a systematic method to search for low-period sinks in a specified region of the parameter space, and report results of applying this method to the region $Q_0 = [1.3999, 1.4001] \times [0.2999, 0.3001]$. The method is based on finding a carefully selected set of periodic orbits existing for fixed parameter values, and then using continuation in the parameter space to find a sink. This approach allows us to find many more periodic windows, and in consequence find sinks for parameter values much closer to the classical case, than using the monitoring trajectory based method.⁴ We will prove that in a neighbourhood of the classical parameter values, there is an abundance of periodic windows of moderately low periods. As an example, we have the following result:

relatively large periods. Moreover, for this method, certain improvements based on symbolic representations of periodic windows are possible, which significantly reduce time necessary to find all periodic orbits of a given period.

The Biham–Wenzel method to find period- p cycles of h is based on the construction of artificial continuous dynamical systems of order p defined by

$$\frac{dw_k}{dt} = s_k \left(-w_{(k+1) \bmod p} + a - w_k^2 + bw_{(k-1) \bmod p} \right), \quad (2)$$

for $0 \leq k < p$, where $(w_0, w_1, \dots, w_{p-1})$ is the state vector and $s = (s_0, s_1, \dots, s_{p-1})$ is a symbol sequence with $s_k \in \{-1, +1\}$. To shorten the notation, we will use only signs to denote a particular sequence. For longer sequences, we will use powers to denote a sequence composed of repeated subsequences. For example, we will write $(- - - + +)$ or $(-^3 +^2)$ to denote the sequence $(-1, -1, -1, +1, +1)$.

Note that if $(z_0, z_1, \dots, z_{p-1})$ is a periodic orbit of h with $z_k = (x_k, y_k)$, then $(w_0, w_1, \dots, w_{p-1})$ defined by $w_k = ax_k$ satisfies $-w_{(k+1) \bmod p} + a - w_k^2 + bw_{(k-1) \bmod p} = 0$ for all $0 \leq k < p$. This can be seen by noting that $w_{(k+1) \bmod p} = ax_{(k+1) \bmod p} = a(1 - ax_k^2 + bx_{(k-1) \bmod p}) = a - w_k^2 + bw_{(k-1) \bmod p}$. It follows that there is a one-to-one correspondence between fixed points of h^p and equilibria of (2). In Ref. 5, it is claimed that for each fixed point of h^p , there is exactly one symbol sequence s for which the corresponding equilibrium of (2) is stable. This claim is not always true. In fact, in Ref. 12, several examples where the method fails to find existing orbits are given. Theoretical foundations for the Biham–Wenzel method and discussion under what conditions the method is capable of finding all periodic orbits are given in Ref. 13. Symbol sequences for which periodic orbits exist are called *admissible*. If the region of interest in parameter space is small, then usually only a small fraction of admissible sequences correspond to periodic windows intersecting this region. In Sec. III, we describe methods to reduce the number of sequences for which the continuation method is applied. This improvement will be essential for the successful application of the search procedure.

In what follows, we do not rely on that the method always works properly, for our purpose it is sufficient that the method is capable of finding a majority of periodic orbits with a given period. In order to find fixed points of h^p , it is proposed in Ref. 5 to locate steady state behaviors for all possible symbol sequences of length p . The system (2) is integrated until either the right hand side of (2) becomes sufficiently small (it is proposed to use the value $\varepsilon = 10^{-7}$) or the norm of the solution w_k becomes sufficiently large. The first case suggests that a periodic orbit of h has been found; the second case indicates that the solution escapes to infinity. If an equilibrium is stable, a trajectory converges to it for initial conditions which are small with respect to \sqrt{a} (in the following we use initial conditions $w_k = 0$). Since we are only interested in steady states, we use a simple integration method with a relatively large time step; the fourth-order Runge–Kutta method with step size 1/10.

The procedure described above can be used to locate periodic orbits of a given period for given parameter values. Most of these found periodic orbits (usually all) are unstable.

In the next step, for each admissible symbol sequence, we use the continuation method to find a point in the parameter space where the periodic orbit becomes stable. The search is carried out in the direction $-(\partial\sigma/\partial a, \partial\sigma/\partial b)$, where σ is the spectral radius of the Jacobian matrix $(h^p)'$ (for details how to compute the Jacobian matrix, its eigenvalues, derivatives of eigenvalues with respect to parameters, and how to find new position of the orbit when moving in the parameter space see Ref. 4). When at a certain point obtained during the continuation procedure the spectrum of the Jacobian matrix is within the unit circle, the procedure is stopped—the periodic window has been found. If the continuation procedure leads outside the region of interest, it is also stopped with no sink. In the former case, we may continue the sink to find the region where the sink exists. Such a region in the parameter space will be called a *periodic window*. Various versions of the continuation method for finding periodic windows are presented in Refs. 11 and 4.

C. Confirming the existence of a sink

Once we have a candidate for a sink, we can prove its existence using interval arithmetic tools.^{14,15} This is done to ensure that the sink found is not a rounding error artifact. To investigate zeros of $F : \mathbb{R}^n \mapsto \mathbb{R}^n$ in the interval vector \mathbf{x} , one evaluates an interval operator, for example, the interval Newton operator,¹⁵ over \mathbf{x}

$$N(\mathbf{x}) = \hat{x} - F'(\mathbf{x})^{-1}F(\hat{x}), \quad (3)$$

where $\hat{x} \in \mathbf{x}$ and $F'(\mathbf{x})$ is an interval matrix containing the Jacobian matrices $F'(x)$ for all $x \in \mathbf{x}$. The main theorem on the interval Newton operator states that if $N(\mathbf{x}) \subset \mathbf{x}$, then F has exactly one zero in \mathbf{x} .

To study the existence of period- p orbits of h , we construct the map $F : \mathbb{R}^p \mapsto \mathbb{R}^p$ defined by

$$[F(x)]_k = 1 - ax_k^2 + bx_{(k-1) \bmod p} - x_{(k+1) \bmod p}, \quad (4)$$

for $k = 0, 1, \dots, p - 1$. $x = (x_0, x_1, \dots, x_{p-1})$ is a zero of F , and only if $z_0 = (x_0, y_0) = (x_0, bx_{p-1})$ is a fixed point of h^p .

To prove the existence of a periodic orbit in a neighborhood of the computer generated trajectory $x = (x_0, x_1, \dots, x_{p-1})$, we choose the radius r , construct the interval vector $\mathbf{x} = (x_0, x_1, \dots, x_{p-1})$, where $x_k = [x_k - r, x_k + r]$, and verify whether $N(\mathbf{x}) \subset \mathbf{x}$. If the existence condition does not hold, we may choose a different r and try again.

The stability of the orbit $z = (z_0, z_1, \dots, z_{p-1})$ depends on the eigenvalues $\lambda_{1,2}$ of the Jacobian matrix

$$J_p(z_0) = (h^p)'(z_0) = h'(h^{p-1}(z_0)) \cdots h'(h(z_0)) \cdot h'(z_0), \quad (5)$$

where $z_0 = (x_0, y_0) = (x_0, bx_{p-1})$. We will assume that the eigenvalues are ordered in such a way that $|\lambda_1| \geq |\lambda_2|$. If both eigenvalues lie within the unit circle, i.e., $|\lambda_1| < 1$, then the orbit is asymptotically stable. If at least one eigenvalue lies outside the unit circle ($|\lambda_1| > 1$), then the orbit is unstable.

Note that the determinant of the Jacobian matrix of the Hénon map is $\det(h'(x, y)) = -b$. It follows that $\lambda_1 \lambda_2 = \det(J_p(z_0)) = (-b)^p$, so $|\lambda_2| < 1$ for $|b| < 1$.

III. SEARCH RESULTS

In this section, we present results from our search for periodic windows intersecting the square $Q_0 = 1.4001 \times 0.2999$. We start by finding periodic orbits existing for the classical parameter values.

A. Periodic orbits for $(a^*, b^*) = (1.4, 0.3)$

In order to locate period- p orbits using the Biham–Wenzel method, we consider symbol sequences of length p . There are 2^p such sequences. Eliminating cyclic permutations and sequences for which the primary period is not p reduces the number of sequences to be considered by at least a factor of p . For example, when $p = 33$, the number of sequences to be considered is $260300986 \approx 2.6 \times 10^8$, while the total number of sequences of length 33 is $2^{33} \approx 8.6 \times 10^9$. The number of sequences can be further decreased by skipping sequences containing forbidden subsequences (compare also the idea of pruning¹⁶). It has been found that for (a^*, b^*) admissible sequences of length $p \leq 33$ apart from the fixed point with symbol sequence $s = (-)$ located outside the numerically observed attractor do not contain subsequences $(- - -)$, $(- + + -)$, and $(- - + -)$. This property has also been confirmed for all four corners of Q_0 . This suggests that these three subsequences are *forbidden* and we can exclude sequences containing them when searching for periodic orbits within Q_0 , which greatly reduces the number of sequences to be considered. For example, for $p = 33$, the number of sequences is reduced from 2.6×10^8 to 9.02×10^5 . Even further savings in computation time can be achieved by skipping longer forbidden subsequences. We have verified that 61977 out of $2^{16} = 65536$ subsequences of length 16 do not appear in any admissible sequence of period $p \leq 33$. As before, the sequence $(-)$ corresponding to one of the fixed points was excluded. The set of 61977 forbidden subsequences of length 16 can be simplified to 28 subsequences of various length not larger than 16. Skipping these forbidden subsequences when searching for period-33 orbits decreases the number of sequences to be considered to 2.59×10^5 . Note that it is difficult to further reduce computation time by a substantial factor, since the number of admissible sequences of period-33 is approximately 1.4×10^5 (the exact number depends on the point in Q_0).

In Table I, we report results obtained using the Biham–Wenzel method for $p \leq 50$ for the classical parameter values. Results for $p \leq 28$ have been presented in Ref. 5. We show the number P_p of period- p orbits, and the estimate $H_p = p^{-1} \log F_p$ of the topological entropy of the Hénon map based on the number F_p of fixed points of h^p . The results shown in Table I agree with the rigorous results for $p \leq 30$ presented in Ref. 6, which means that the Biham–Wenzel method works properly for relatively large periods. Let us note that the estimate H_p of the topological entropy stabilizes around 0.46493. The five most significant digits are constant for $p \geq 36$. Based on these results, we could—as a by-product of our search procedure—conjecture that the topological entropy of the Hénon map with classical parameter values belongs to the interval 0.4649_3^4 .

TABLE I. The number of period- p orbits P_p for the Hénon map found using the Biham–Wenzel method for (a^*, b^*) , the estimate H_p of the topological entropy based on the number of fixed points of h^p .

p	P_p	H_p	p	P_p	H_p
18	233	0.4643313	35	333 558	0.4649406
19	364	0.4653622	36	516 064	0.4649374
20	535	0.4644021	37	799 372	0.4649324
21	834	0.4653556	38	1 238 950	0.4649344
22	1225	0.4639811	39	1 921 864	0.4649326
23	1930	0.4652528	40	2 983 342	0.4649381
24	2902	0.4648152	41	4 633 278	0.4649353
25	4498	0.4652113	42	7 200 563	0.4649381
26	6806	0.4648472	43	11 195 444	0.4649353
27	10 518	0.4650695	44	17 418 122	0.4649374
28	16 031	0.4648548	45	27 110 040	0.4649351
29	24 740	0.4649474	46	42 220 339	0.4649365
30	37 936	0.4648635	47	65 779 244	0.4649354
31	58 656	0.4649495	48	102 536 942	0.4649364
32	90 343	0.4649279	49	159 895 912	0.4649358
33	139 674	0.4649578	50	249 454 412	0.4649364
34	215 597	0.4649386			

Similar computations for $p \leq 47$ have been performed for points in the parameter space being corners of the square Q_0 . These results will be used in Sec. III B to find periodic windows having non-empty intersection with the square Q_0 . Estimates of the topological entropy based on the number of short periodic orbits are plotted in Fig. 1. Note that increasing both a and b increases the topological entropy of the Hénon map. For $(a,b) = (1.3999, 0.2999)$ and $(a,b) = (1.4001, 0.3001)$, the entropy estimates oscillate around 0.46480 and 0.46503, respectively. On the other hand, the entropy for the other corners of Q_0 is close to that of the center. Note that the entropy estimates along the interval between $(1.3999, 0.3001)$ and $(1.4001, 0.2999)$ are not monotonic. At the center (a^*, b^*) of this interval, the entropy estimate is larger than at the endpoints.

We would like to stress that although the results obtained using the Biham–Wenzel method agree with the true results for periods $p \leq 30$, we cannot treat this method as a rigorous one. We have observed that the number of periodic orbits found depends on the parameters of the method.

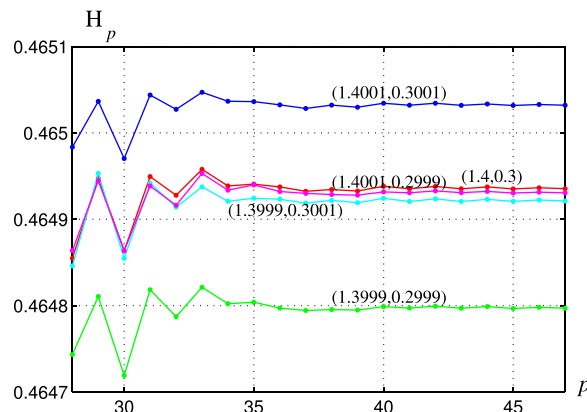


FIG. 1. Estimates $H_p = p^{-1} \log F_p$ of the topological entropy based on the number F_p of fixed points of h^p for different points (a, b) .

For example, the period-33 sequence $s = (-^3+^3 - + - + - + -^2+^3 - + - + - +^3-^2+^4 - +)$ was found admissible for $a = 1.4001$, $b = 0.3001$ when $\varepsilon = 10^{-7}$ was used, and non-admissible for $\varepsilon = 10^{-8}$. The reason for this behaviour is the fact that the region of existence of the periodic orbit with the symbol sequence s starts very close to the point $(1.4001, 0.3001)$.

B. Sink regions intersecting the square

$$Q_0 = 1. \overset{4001}{3999} \times 0. \overset{3001}{2999}$$

In this section, we show how to locate sink regions intersecting the square Q_0 using low-period cycles existing for certain points in the parameter space.

There are two possible approaches to achieve this goal. The first one is to continue all periodic orbits found in the previous step. Continuation is carried out in a direction in which the spectral radius of the Jacobian matrix computed along the periodic orbit decreases, until either a point belonging to the periodic window is found or we leave Q_0 . Since the number of period- p orbits grows fast with p , and the continuation procedure is computationally more expensive than the Biham–Wenzel method, this approach becomes infeasible for larger p .

In the second approach, we find symbol sequences which are admissible at some corners of Q_0 but not all. Such sequences will be referred to as *missing sequences*. For each missing sequence, we continue from a point where this sequence is admissible to find the corresponding periodic window. In a case when the sequence is admissible in more than one corner, we start the continuation procedure at a corner where the search direction points inside Q_0 .

Let us explain why the second approach allows us to find the majority of periodic windows intersecting Q_0 . Recall how periodic orbits emerge in the parameters space. In the fold bifurcation, a pair of periodic orbits are born. For the Hénon map, one of them is stable and the other is unstable. In the period-doubling bifurcation, a periodic orbit loses its stability and a stable orbit with twice the period is born. Hence, one can expect that the region where the orbit is stable is located along the border of the periodic orbit existence region. Therefore, to find periodic windows, we need to detect borders of periodic orbit existence regions. Usually, if the border of existence region intersects Q_0 , the corresponding symbol sequence is admissible for some but not all corners of Q_0 . This happens in most situations because—locally—the existence regions close to the border look like half-planes, and Q_0 is small. Hence, intersections of borders and Q_0 are usually either empty or are (almost) straight intervals. Situations when the border of an existence region turns inside Q_0 are rare (three such examples are given in Ref. 4), which means that the proposed method detects the majority of periodic orbit existence regions intersecting Q_0 .

The number M_p of missing sequences of length p found for Q_0 versus p is shown in Table II. No missing sequences with period $p < 18$ have been found. Since the number of missing sequences is significantly smaller than the number of admissible sequences (compare Table I), the second approach is much faster than the first one.

TABLE II. The number M_p of missing sequences of length p and the number R_p of period- p windows in Q_0 .

p	M_p	R_p	d_p	p	M_p	R_p	d_p
18	2	1	1.125×10^{-5}	30	412	206	3.792×10^{-7}
19	4	2	7.908×10^{-5}	31	624	312	2.153×10^{-8}
20	6	3	7.528×10^{-6}	32	1014	507	3.155×10^{-7}
21	4	2	1.113×10^{-5}	33	1654	827	3.704×10^{-7}
22	10	5	2.462×10^{-6}	34	2580	1290	4.815×10^{-8}
23	10	5	3.899×10^{-5}	35	4192	2096	1.277×10^{-7}
24	24	12	6.259×10^{-6}	36	6545	3273	8.628×10^{-8}
25	34	17	2.035×10^{-6}	37	10510	5255	1.533×10^{-8}
26	60	30	5.185×10^{-6}	38	16582	8293	2.126×10^{-8}
27	110	55	6.421×10^{-6}	39	26594	13298	3.878×10^{-9}
28	160	80	1.969×10^{-8}	40	42114	21061	2.143×10^{-9}
29	248	124	1.465×10^{-6}	41	67514	33756	4.728×10^{-10}

For all missing sequences with period $p \leq 41$, the corresponding periodic orbits have been continued to find periodic windows. The results are shown in Table II. We report the number R_p of period- p windows found in Q_0 and the distance d_p between the closest period- p window and the point (a^*, b^*) . In each case, the existence of a sink was proved using the interval Newton method. The total number of detected sink regions with period $p \leq 41$ is 90510, which is significantly more than 461 periodic windows found using the monitoring trajectory approach (compare Ref. 4). Note that the number of missing sequences and the number of periodic windows grow exponentially with the period, as expected.

For odd p , periodic orbits are created via the fold bifurcation, and hence, we expect that half of the missing sequences correspond to periodic windows, i.e., $M_p = 2R_p$. For even p in a given region, we expect $R_{p/2}$ period- p windows created via period-doubling bifurcations. The remaining orbits are created via fold bifurcations, and hence, $M_p = R_{p/2} + 2(R_p - R_{p/2}) = 2R_p - R_{p/2}$. Therefore, one can expect that the following relation between the number of missing sequences and the number of periodic windows holds:

$$M_p = \begin{cases} 2 \cdot R_p & \text{if } p \text{ is odd,} \\ 2 \cdot R_p - R_{p/2} & \text{if } p \text{ is even.} \end{cases} \tag{6}$$

Note that the above relation is satisfied by data in Table II for $p < 38$. For $p = 38, 39, 40, 41$, the difference between the value of M_p calculated using (6) and the actual value is 2, 2, 5, and -2, respectively. This may be caused by the fact that for larger p , there are more borders of periodic orbit existence regions passing close to the corners of Q_0 which may cause a failure of the Biham–Wenzel method.

212 periodic windows with periods $p \leq 28$ are plotted in Fig. 2. These periodic windows have been found using a version of the continuation method designed for narrow regions described in detail in Ref. 4. All periodic windows with periods $p \leq 22$ are labeled.

Each minimal distance between a periodic window and (a^*, b^*) is shown in Fig. 3. Note that the closest period-28 window passes at an exceptionally small distance of 2.3×10^{-8} when compared to periodic windows with similar

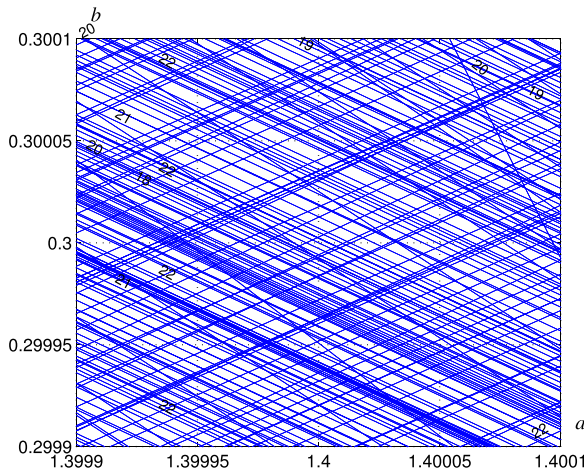


FIG. 2. Periodic windows with periods $p \leq 28$.

or smaller periods. All other periodic windows with periods $p \leq 36$ are at a larger distance. This periodic window was the closest one found using the brute force approach.⁴

The distance d_p between the closest period- p window and (a^*, b^*) generally decreases when p grows (compare also Table II). The closest periodic window corresponds to the period-41 symbol sequence $(-^3+^4 - +^3 -^2+^4 -^2+^4 -^2+^3 - + - +^9)$. We have verified that the point $a = 1.3999999997706479$, $b = 0.29999999958655875$ belongs to this window. The distance between this point and (a^*, b^*) is less than 4.728×10^{-10} , which is approximately 60 times less than for the closest periodic window reported in Ref. 4.

C. Periodic windows intersecting $I_1 = 1.\overset{40000001}{39999999} \times 0.3$

With the goal of finding a periodic window as close to the classical values as possible, we have carried out similar computations for $p \geq 42$ on a much smaller region in the parameter space. Decreasing the size of the region reduces the number of missing sequences, and thus shortens the computation time needed to handle each given p . Missing sequences are identified for the endpoints of the interval $I_1 = 1.\overset{40000001}{39999999} \times 0.3$ of length 2×10^{-8} . For each missing sequence, the corresponding periodic orbit is continued from the point where this sequence is admissible along the interval I_1 toward a sink. The number R_p of periodic windows found

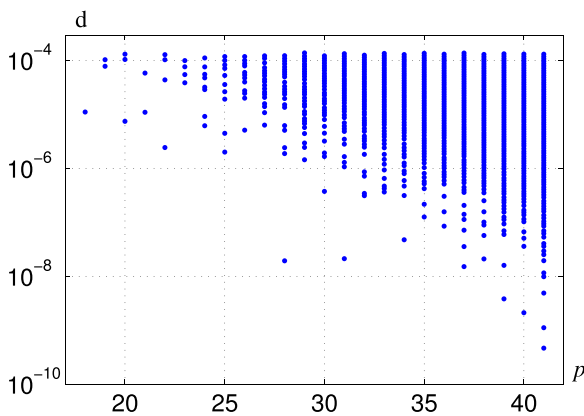


FIG. 3. Distances between period- p windows intersecting Q_0 and (a^*, b^*) .

is reported in Table III. We also give an upper bound of the distance between the closest period- p window and the point (a^*, b^*) .

A total of 465 periodic windows with periods $p \leq 52$ intersecting I_1 have been found. No periodic window with period smaller than 39 was found. The closest periodic window was found for the period-52 symbol sequence $(-^3+^4 - +^3 -^2+^7 - + - + -^2+^6 - +^5 - + - +^3 - +^5 - +)$. The point $a = 1.40000000002152529358126$, $b = 0.30000000000388157716514978$ belongs to this periodic window. The distance between this point and (a^*, b^*) is less than 4.439×10^{-12} and is more than 100 times smaller than the closest period-41 window found in the previous search.

Assuming that sink windows intersect the interval I_1 at random positions, one can estimate what period p should be considered to find a periodic window closer than ε from a given point with a given probability. Based on the data presented in Table III for $45 \leq p \leq 52$, a linear regression model for $\log(R_p)$ versus p has been computed. Using this model, the number of period- p windows intersecting I_1 can be approximated as

$$R_p \approx R_0 q^p, \tag{7}$$

where $q = 1.6115$ and $R_0 = 3.0062 \cdot 10^{-9}$. Note that q is close to $e^H \approx 1.592$, where $H = 0.46493$ is an approximation of the topological entropy of the Hénon map for (a^*, b^*) .

For $p > 52$, the number of periodic windows with periods not larger than p intersecting I_1 can be approximated as $R_{\leq p} = R_{\leq 52} + R_0 q^{53} (q^{p-53+1} - 1) / (q - 1)$, where $R_{\leq 52} = 465$ is the number of period- p windows found for $39 \leq p \leq 52$. The probability that at least one of N points selected randomly with uniform distribution from the interval I_1 of length $l = 2r = 2 \times 10^{-8}$ falls within the selected interval of length 2ε is $P(N) = 1 - ((l - 2\varepsilon)/l)^N = 1 - (1 - \varepsilon/r)^N$. Assuming $P(N) \geq 0.5$ and solving for N yields $N \geq N_\varepsilon = \log 0.5 / (\log(1 - \varepsilon/r))$. Solving the inequality $R_{\leq p} \geq N_\varepsilon$, we obtain

$$p \geq 52 + \frac{\log\left(\frac{(q-1)(N_\varepsilon - R_{\leq 52})}{R_0 q^{53}} + 1\right)}{\log q} \approx \frac{\log\left(\frac{(q-1)\log 2r}{q R_0 \varepsilon}\right)}{\log q}. \tag{8}$$

TABLE III. The number R_p of period p windows intersecting the interval $I_1 = 1.\overset{40000001}{39999999} \times 0.3$, and the distance d_p between the closest period- p window and the point (a^*, b^*) .

p	R_p	d_p	p	R_p	d_p
39	1	3.813×10^{-9}	46	9	3.609×10^{-10}
40	1	2.143×10^{-9}	47	18	1.909×10^{-11}
41	3	4.728×10^{-10}	48	28	5.832×10^{-11}
42	3	1.089×10^{-9}	49	50	4.144×10^{-11}
43	1	2.581×10^{-9}	50	71	1.165×10^{-10}
44	4	1.457×10^{-9}	51	109	4.700×10^{-11}
45	6	3.012×10^{-10}	52	161	4.439×10^{-12}

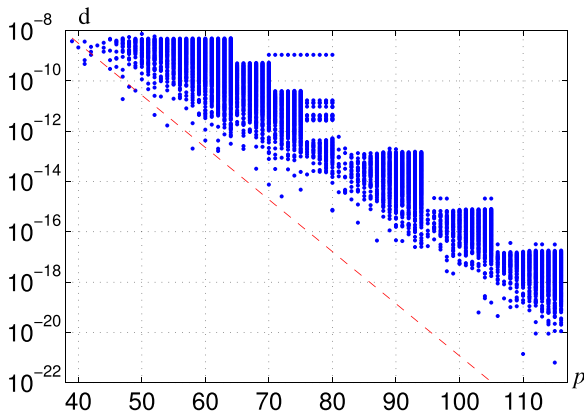


FIG. 5. Distances between period- p windows intersecting I_1 and (a^*, b^*) .

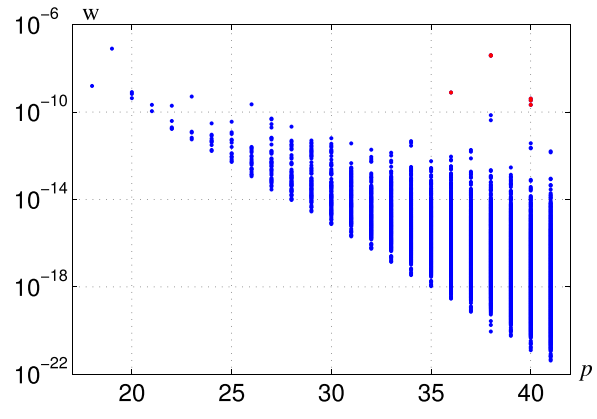


FIG. 6. Periodic window width versus period p .

in such a group are located in a small region not containing the point (a^*, b^*) . They correspond to non-optimal selections of subsequences. Generally, the minimum distance decreases exponentially with the increase of p . 57 periodic windows within the distance 10^{-19} , and four within the distance 10^{-20} from (a^*, b^*) were found. This shows that the selection method based on choosing subsequences present frequently in sequences corresponding to closest periodic windows found so far works well.

The relation between p and ε presented in (8) is plotted in Fig. 5 as a dashed line. It shows what minimum distance ε we can expect by considering symbol sequences of length not larger than p . Let us note that for $p \leq 62$, the distance of the closest periodic window found oscillates around the approximation $\varepsilon(p)$. For larger p , the minimum distances are larger than $\varepsilon(p)$, which is perhaps caused by skipping some non-forbidden sequences. Thus, we can expect that, for $p > 62$, there exist periodic windows closer to $(1.4, 0.3)$ than the ones reported here.

IV. IS THE HÉNON ATTRACTOR CHAOTIC

In Secs. III B and III C, we have shown several examples of periodic windows very close to the classical parameter values (a^*, b^*) . We considered all non-forbidden periodic symbol sequences of length $p \leq 52$ and selected symbol sequences of length $53 \leq p \leq 116$. From the results obtained, it follows that there might exist a sequence for which the corresponding periodic window encloses the point (a^*, b^*) . In this section, we estimate that the probability that the Hénon attractor (the attractor existing for classical parameter values) is periodic.

First, let us estimate the area of the periodic windows in the square $Q_0 = [1.4001, 1.3999] \times [0.3001, 0.2999]$. Fig. 6 shows widths of the existence regions intersecting Q_0 versus period. Period-doubling windows are plotted using a different color. The width of a periodic window is found by continuing the sink from the point in the parameter space for which the existence was proved in the directions $\pm(\partial\sigma/\partial a, \partial\sigma/\partial b)$, where σ is the spectral radius of the Jacobian matrix $(h^p)'$. Continuation is carried out until both eigenvalues of the Jacobian matrix are smaller than 1 in magnitude. This procedure gives us two border points and the window width is their distance.

The two widest windows are period-19 windows with widths of 7.96×10^{-8} and 7.62×10^{-8} . In the plot, they are visible as a single point. Observe the period-36, period-38, and period-40 period-doubling windows have widths a couple of orders of magnitude larger than other windows with the same periods. In fact, the widths of period-doubling windows are only slightly smaller than widths of their parents. The width of a primary window generally decreases exponentially with the period.

Having widths of periodic windows with a period p , we can estimate the area of intersection of period- p windows with the square Q_0 . This estimate is based on the assumption that the intersections of periodic windows with Q_0 are narrow stripes, and that the width of the stripe is almost constant in Q_0 . In Ref. 4, it was confirmed that both assumptions are valid for the majority of periodic windows found. The direction of the periodic window is approximately $(\partial\lambda_1/\partial b, -\partial\lambda_1/\partial a)$. Having the direction and a point belonging to the periodic window, we can compute the length of the intersection of the periodic window and Q_0 , and then its area.

Fig. 7 shows the total area $S_{all,p}$ of period- p windows enclosed in Q_0 . Note that the results for even periods $p \geq 36$ are much larger than for odd periods in the same range. As it was explained before, this is caused mainly by the existence of period-doubling windows for these periods. The total area

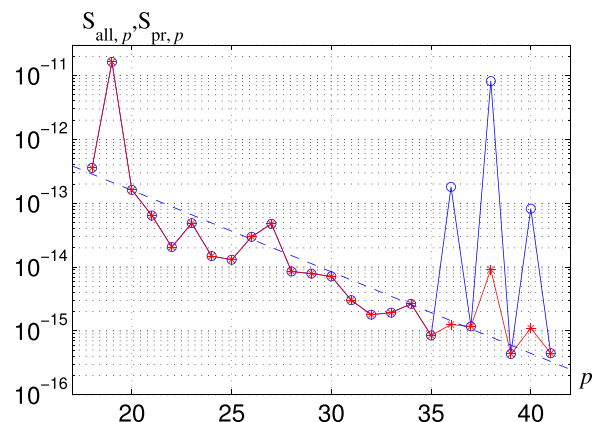


FIG. 7. The total area $S_{all,p}$ of period- p windows enclosed in Q_0 (symbol \odot), and the total area $S_{pr,p}$ of primary period- p windows enclosed in Q_0 (symbol \star).

$S_{pr,p}$ of period- p primary windows in Q_0 is plotted using the \ast symbol. $S_{pr,p}$ fluctuates much less for $p \geq 36$ than $S_{all,p}$. The linear regression model of $\log(S_{pr,p})$ is shown as a dashed line. The model $S_{pr,p} = S_0 q^p$ has parameters $S_0 = 5.68 \times 10^{-11}$, $q = 0.745$. Based on this model, we can estimate that the total area of primary periodic windows with $p \geq 42$ is close to $S_{pr,42+} \approx S_0 q^{42} / (1 - q) \approx 9.73 \times 10^{-16}$.

Let us further assume that each primary period- p window generates an infinite cascade of period-doubling windows with periods $2^k p$, and that the ratios $\alpha_k = w_{2^{k-1}p} / w_{2^k p}$ of the widths of subsequent windows are similar for all cascades. We will estimate the values of α_k based on the analysis of selected sequences of periodic windows in Q_0 . The widths of the period-18 window and its descendants are $w_{18} \approx 3.207 \times 10^{-9}$, $w_{36} \approx 1.604 \times 10^{-9}$, $w_{72} \approx 3.788 \times 10^{-10}$, and $w_{144} \approx 8.322 \times 10^{-11}$. Each width is calculated along the line $b = 0.3$. The ratios of the widths of subsequent windows are: $\alpha_1 = w_{36} / w_{18} \approx 0.50002$, $\alpha_2 = w_{72} / w_{36} \approx 0.23620$, and $\alpha_3 = w_{144} / w_{72} \approx 0.21972$. For one of the period-19 windows and its descendants, we obtain $w_{19} \approx 9.402 \times 10^{-8}$, $w_{38} \approx 4.733 \times 10^{-8}$, $w_{76} \approx 1.118 \times 10^{-8}$, and $w_{152} \approx 2.457 \times 10^{-9}$. In this case, all widths are calculated along the line $a = 1.4$ (the period-19 window does not intersect the line $b = 0.3$ within Q_0). The ratios of the widths of the subsequent windows are: $\alpha_1 = w_{38} / w_{19} \approx 0.50335$, $\alpha_2 = w_{76} / w_{38} \approx 0.23622$, and $\alpha_3 = w_{152} / w_{76} \approx 0.21976$. The ratios α_k calculated in both cases are very close. Similar results were obtained for other period-doubling cascades. Note that α_3 is quite close to the inverse of the Feigenbaum constant $\delta^{-1} \approx 0.21417$. We expect that—in the limit—the ratio α_k converges to δ^{-1} . Assuming that $\alpha_1 \approx 0.5$, $\alpha_2 \approx 0.2362$, $\alpha_3 \approx 0.2198$, and $\alpha_k \approx \delta^{-1}$ for $k > 3$, we can estimate the width of all descendants as $\beta = \alpha_1(1 + \alpha_2(1 + \alpha_3(1 + \delta^{-1}/(1 - \delta^{-1})))) = 0.6511$ of the width of a primary window.

Therefore, we can estimate the total area of all periodic windows in Q_0 as

$$S_{all} \approx \sum_{p=18}^{41} S_{all,p} + \sum_{p=21}^{41} \left(\beta S_{pr,p} + \frac{\beta - \alpha_1}{\alpha_1} S_{pd,p} \right) + (1 + \beta) S_{pr,42+} = 2.835 \times 10^{-11}.$$

The first component corresponds to the area of all periodic windows identified by the search procedure. It is equal to 2.5607×10^{-11} and dominates the other two components. The second component approximates the area of period-doubling descendants of periodic windows found. Note that the sum starts at $p = 21$. The reason is that period-doubling children of period-18, 19, and 20 periodic windows are already accounted for in the first component. Also note that primary windows and period-doubling windows are treated in a different way. The second component is equal 2.737×10^{-12} and is approximately nine times smaller than the first one. The last component estimates the area of primary windows with periods $p \geq 42$ and their period-doubling descendants. This component is equal to 1.606×10^{-15} and has a negligible influence on the result. Formally, we should subtract from S_{all} the area of

intersections of periodic windows. This area is, however, a couple of magnitudes smaller than the area of S and has negligible effect on the result.

Dividing S_{all} by the area of Q_0 , we obtain the probability that a randomly selected point in Q_0 belongs to a periodic window

$$P_{per,Q_0} \approx S_{all} / S_{Q_0} = 7.09 \times 10^{-4}. \tag{9}$$

Let us assume that all periodic windows with periods smaller than 42 are found. This assumption may be not true due to several reasons. Some of the windows may be not found due to a failure of the Biham–Wenzel method. It is also expected that there exist periodic windows for which the intersection with Q_0 is a more complex structure than a narrow stripe, in which case the proposed method may be not able to detect it. However, we believe that the majority of periodic windows with periods smaller than 42 have been found. From the analysis of distances between periodic windows found and the point (a^*, b^*) , we know that period-doubling descendants of periodic windows with periods $p \leq 41$ do not contain the point (a^*, b^*) . The probability that the point (a^*, b^*) belongs to a periodic window not found by the search procedure then drops to

$$P_{per42+,Q_0} = (1 + \beta) \cdot S_{pr,42+} / S_{Q_0} = 4.02 \times 10^{-8}. \tag{10}$$

Similar computations have been carried out for the interval $I_0 = 1.3999 \times 0.3$. The Biham–Wenzel method was used to find admissible sequences with periods $p \leq 42$ for points $(1.3999, 0.3)$ and $(1.4001, 0.3)$, the missing sequences have been identified, and the continuation method was used for periodic orbits corresponding to missing sequences to find intersections of periodic windows with I_0 . The total width $W_{all,p}$ of intersections is shown in Fig. 8. The total width $W_{pr,p}$ of period- p primary windows in I_0 is plotted using the \ast symbol. The linear regression model of $\log(W_{pr,p})$ is shown as a dashed line. The model $W_{pr,p} = W_0 q^p$ has parameters $W_0 = 1.6914 \times 10^{-7}$, $q = 0.744$. Note that the second parameter of the model is almost equal to the corresponding parameter for the model of area of periodic windows in Q_0 . Based on these results and the model, we can estimate the

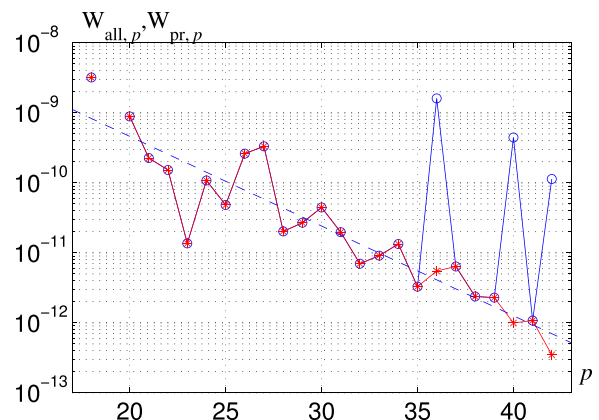


FIG. 8. The total width $W_{all,p}$ of period- p windows intersecting I_0 (symbol \odot), and the total width $W_{pr,p}$ of primary period- p windows intersecting I_0 (symbol \ast).

total width $W_{\text{all}} \approx 8.92 \times 10^{-9}$, and the probability that a randomly selected point from I_0 belongs to a periodic window as $P_{\text{per},I_0} \approx W_{\text{all}}/W_{I_0} = 4.46 \times 10^{-5}$. This probability is smaller than the probability (9). The main reason is the existence of two wide period-19 windows which intersect Q_0 without intersecting I_0 (compare Fig. 2).

Similarly, as for Q_0 , we can estimate the probability that the point (a^*, b^*) belongs to a periodic window not found by the search procedure $P_{\text{pr},43+,I_0} = (1 + \beta) \cdot W_{\text{pr},43+}/W_{I_0} = 1.68 \times 10^{-8}$. This result is consistent with (10). A slightly lower value is the effect of period-19 windows not intersecting I_0 and the fact that here the results are based on periodic windows with periods $p \leq 42$ instead of $p \leq 41$ for Q_0 .

The results obtained for the interval I_1 concerning periodic windows with periods $p \leq 52$ can be used in a similar way to estimate the probability that the point (a^*, b^*) belongs to a period- p window with $p \geq 53$

$$P_{\text{per},53+,I_1} = (1 + \beta) \cdot W_{\text{pr},53+}/W_{I_0} = 4.59 \times 10^{-11}. \quad (11)$$

This already very low probability can be further decreased by considering smaller neighborhoods of (a^*, b^*) and longer symbol sequences.

From the results presented above, it follows that the probability of the Hénon attractor being periodic is extremely low. Hence, the general belief that the Hénon attractor is chaotic is perhaps true. However, taking into account that there exist periodic windows extremely close to the point (a^*, b^*) (perhaps arbitrarily close), it seems very unlikely that one could ever rigorously confirm this hypothesis.

A. Sink properties

To investigate sink properties, we will use the notion of the immediate basin of attraction and its radius.⁴ We say, that a point z belongs to the *immediate basin of attraction* $B_\varepsilon(A)$ of the attractor A if its trajectory converges to the attractor and does not escape further than ε from it

$$B_\varepsilon(A) = \{z : d(h^n(z), A) \leq \varepsilon \forall n \geq 0 \text{ and } \lim_{n \rightarrow \infty} d(h^n(z), A) = 0\},$$

where $d(z, A)$ denotes the distance between the point z and the set A . We will use ε to be 1% of the diameter of the smallest ball enclosing the attractor. The condition $z \in B_\varepsilon(A)$ can be verified numerically by computing the trajectory of z in arithmetic of sufficient precision.

The *immediate basin radius of the attractor* A is defined as

$$r_\varepsilon(A) = \sup\{r : d(z, A) \leq r \Rightarrow z \in B_\varepsilon(A)\}. \quad (12)$$

The border of the immediate basin of attraction of a stable period-18 point existing for $a = 1.3999769102, b = 0.3$ in a neighborhood of this point is shown in Fig. 9. The periodic point is plotted using the \times symbol. The immediate basin radius at this point is the radius of the largest circle centered at the periodic point enclosed in the immediate basin of attraction (see Fig. 9). Sample trajectories are plotted in blue. They give an idea what the potentially chaotic set looks like.

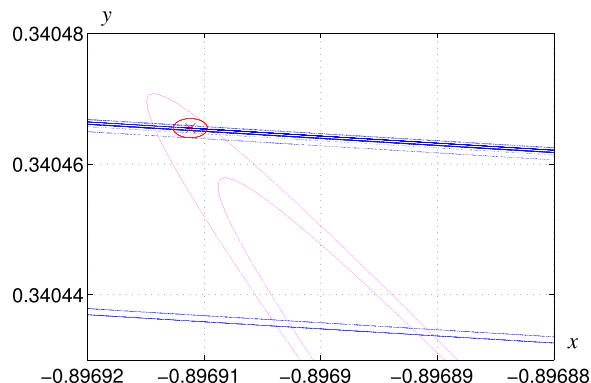


FIG. 9. Immediate basin of attraction of a period-18 sink for $a = 1.3999769102, b = 0.3$.

Computation of $r_\varepsilon(A)$ for periodic attractors is straightforward. One can use a bisection method to obtain an accurate approximation of the largest r such that the condition $z \in B_\varepsilon(A)$ is satisfied for test points in balls of radius r centered at the positions of periodic points constituting the sink.

If the immediate basin radius of a sink is smaller than the arithmetic precision used, a trajectory will most likely escape from the sink even if the computations are started at a stable periodic point; in general we will not be able to observe the sink in simulations (compare Ref. 17). Provided that the computations are carried out in a sufficient precision, a trajectory initiated at a point closer to the sink than its immediate basin radius converges to the sink without leaving its small neighborhood; in simulations we will see a stable periodic behavior.

We will show that the immediate basin radius can be used to estimate the average time needed for a trajectory to converge to the sink. In certain cases, monitoring the trajectory to observe convergence is not an option; convergence times can be prohibitively long.

The immediate basin radius versus period p for periodic windows in Q_0 is plotted in Fig. 10. The immediate basin radius is computed for a point in a periodic window at which the spectral radius of the Jacobian matrix reaches its minimum. The position of the minimum is found using the continuation method. One can see that in several cases for

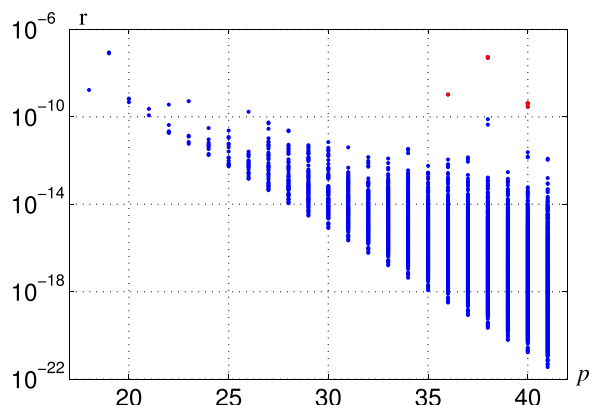


FIG. 10. The immediate basin radius versus period p for periodic windows in Q_0 .

periods larger than 33, the immediate basin radius is smaller than the double precision machine epsilon.

Observe that the plot of the immediate basin radius versus period is very similar to the plot of the periodic window width versus period (compare Fig. 6 and Fig. 10). This is a consequence of the *equivalence of parameter and space derivatives*, which holds for the Hénon map.³ This observation indicates that two effects which increase the difficulty to find a sink happen simultaneously. At the same time, as the width of the existence region decreases (we need finer sampling of the state space to find a periodic window), the minimum immediate basin size of the corresponding sink becomes smaller (we need more iterations to detect the sink in simulations).

Even if there exists a single sink for given parameter values, it may take a very long time to observe any convergence to this sink. In theory, for any number of iterations n , we may find a trajectory which converges to the sink only after more than n iterations. If a trajectory is initiated sufficiently close to one of the infinitely many unstable periodic orbits, the convergence time can be as large as we wish. It follows that convergence times are not bounded. On the other hand, if a trajectory is started right at the sink, or within its immediate basin, we will see no transient behaviour at all. Estimating the average convergence time is an interesting problem. If it is large, then we have little chance of finding the sink observing short trajectories. Let $n_{\text{conv}}(\varrho)$ denote the average number of iterations which are required to converge to the sink with probability $\varrho \in (0, 1)$. This number can be approximated in the following way. First, we compute trajectories for N random initial points and record the corresponding convergence times τ_k . Next, we sort the convergence times $\tau_1 \leq \tau_2 \leq \dots \leq \tau_N$ and find n such that $n/N \approx \varrho$. τ_n is an approximation of $n_{\text{conv}}(\varrho)$. We have carried out such calculations for several sinks; the results are collected in Table V. We report the sink period p , the distance d between the point (a, b) for which the existence has been proved and the point (a^*, b^*) ,

the immediate basin radius r_ε , the width w , and an estimate of $n_{\text{conv}}(0.5)$. The sinks are sorted according to the immediate basin radius. We also report the minimum floating point precision required to observe the sink in simulations. This number is computed as the minimum number of bits of multi-precision arithmetic used such that the computer generated trajectory initiated at the sink does not leave a small neighborhood of the sink.

Note that the ratio d/w for the closest periodic window (period-115) is larger than 10^{29} , which means that this periodic window is very far away from point (a^*, b^*) when the distance is measured in window widths. There is practically no chance to find this window by sampling the parameter space. For comparison, the ratio d/w for the period-18 window is approximately 7200, and for the widest period-19 window, it is close to 1000.

The results concerning immediate basin radius are consistent with the minimum precision results. The first six sinks can be seen when standard double precision arithmetic is employed (53 bits precision in the mantissa). The immediate basin radius for these sinks is larger than the double precision machine epsilon. For the remaining sinks, the double precision arithmetic is not sufficient. For example, the immediate basin radius of the period-41 sink is $r_\varepsilon = 3.31 \times 10^{-17}$. We have verified that this sink appears to be unstable when the computations are performed in standard double precision; a trajectory escapes from the sink even if it started exactly (up to double precision resolution) at the sink position. For the closest period-115 sink, the immediate basin radius is extremely small. In consequence, the quadruple precision arithmetic (128 bits) is not sufficient to detect it.

In the last column of Table V, we report the results concerning approximations of $n_{\text{conv}}(0.5)$. For the first three sinks, the results are based on convergence times for 10^5 randomly selected initial points. For the sinks #4–6 due to longer convergence times, we use fewer initial points. For the remaining sinks the calculations have to be carried out in multiple precision. For the sinks #7 and 8, the results were obtained using multiple precision GPU software.¹⁸ For the other sinks, we were not able to get any significant statistics concerning the convergence times.

Let us try to estimate how the convergence time changes with r_ε . Define the set \mathcal{A} to be the invariant part of a big trapping region Ω enclosing the numerically observed attractor, i.e., $\mathcal{A} = \bigcap_{n=0}^\infty h^n(\Omega)$. For (a^*, b^*) , the trapping region Ω can be chosen as a quadrangle defined by points $(-1.33, 0.42)$, $(1.32, 0.133)$, $(1.245, -0.14)$, and $(-1.06, -0.5)$. Such a set for (a, b) close to (a^*, b^*) supports horseshoe type dynamics, contains an infinite number of periodic orbits, and contains a chaotic set (which may be a repeller). Let us assume that \mathcal{A} is an interval of length L , and that a trajectory visits \mathcal{A} randomly with uniform distribution. The probability that at least one point out of N falls within a ball of radius r from a period- p orbit is $P = 1 - (1 - 2pr/L)^N$. Solving $P = \varrho$ yields

$$N = \frac{\log(1 - \varrho)}{\log\left(1 - \frac{2pr}{L}\right)} \approx \frac{L \log(1 - \varrho)^{-1}}{2pr}. \tag{13}$$

TABLE V. Parameters of selected sinks.

p	d	r_ε	w	Prec.	$n_{\text{conv}}(0.5)$
18	1.12×10^{-5}	1.68×10^{-9}	1.56×10^{-9}	28	3.35×10^6
33	5.13×10^{-7}	7.71×10^{-13}	7.13×10^{-13}	41	1.66×10^9
28	2.25×10^{-8}	1.16×10^{-13}	1.07×10^{-13}	43	1.44×10^{10}
31	1.08×10^{-6}	1.41×10^{-14}	1.38×10^{-14}	47	3.83×10^{10}
31	2.15×10^{-8}	1.73×10^{-15}	1.60×10^{-15}	51	2.35×10^{11}
33	3.70×10^{-7}	6.34×10^{-16}	5.85×10^{-16}	53	2.68×10^{11}
41	4.73×10^{-10}	3.31×10^{-17}	3.31×10^{-17}	55	4.40×10^{12}
47	1.47×10^{-10}	1.17×10^{-20}	1.17×10^{-20}	67	9.07×10^{14}
47	1.91×10^{-11}	1.34×10^{-22}	1.24×10^{-22}	74	
52	4.44×10^{-12}	4.82×10^{-24}	4.44×10^{-24}	80	
58	2.03×10^{-13}	1.55×10^{-26}	1.46×10^{-26}	88	
62	1.64×10^{-13}	2.60×10^{-29}	2.59×10^{-29}	97	
72	2.55×10^{-15}	6.02×10^{-34}	5.63×10^{-34}	113	
80	7.47×10^{-16}	4.62×10^{-37}	4.28×10^{-37}	123	
87	4.52×10^{-17}	3.06×10^{-40}	3.35×10^{-40}	133	
98	2.71×10^{-18}	3.13×10^{-44}	3.17×10^{-44}	147	
103	6.22×10^{-20}	2.45×10^{-46}	2.26×10^{-46}	154	
110	1.38×10^{-21}	2.43×10^{-49}	2.24×10^{-49}	163	
115	6.34×10^{-22}	3.72×10^{-51}	5.49×10^{-51}	170	

For a fixed probability ϱ , the average number of iterations to converge to a period- p sink with immediate basin radius r_ε is inversely proportional to pr_ε .

The assumptions under which the approximation (13) is derived are not valid for the Hénon map. Locally, the set \mathcal{A} has a structure of a Cartesian product of an interval and a Cantor set (compare Fig. 9). Moreover, trajectories do not visit \mathcal{A} according to the uniform distribution. One should also take into account the fact that the immediate basin radius usually changes along the orbit, which means that the true average number of iterations can be larger than (13). In fact, one can see that $n_{\text{conv}}(0.5)$ grows slower than $(pr_\varepsilon)^{-1}$ (compare Table V). Nevertheless, decreasing r_ε from 1.68×10^{-9} to 1.17×10^{-20} corresponds to the increase of $n_{\text{conv}}(0.5)$ from 3.35×10^6 to 9.07×10^{14} . If this trend carries over to smaller r_ε , we have practically no chance of detecting sinks corresponding to periodic orbits with periods larger than say, $p = 100$ by monitoring trajectories. For these sinks, r_ε is below 10^{-45} and the expected number of iterations to converge to a sink is well above 10^{30} .

V. CONCLUSION

The results obtained provide numerical support for the belief that the set of parameter values with a periodic sink is dense in a neighborhood of $(a^*, b^*) = (1.4, 0.3)$. By analogy with the quadratic map, it is also expected that in a neighborhood of (a^*, b^*) the set of parameter values with chaotic behaviour is a Cantor set with positive Lebesgue measure. It has been confirmed that in a neighborhood of (a^*, b^*) ,

periodic windows are very narrow, the transient times to corresponding sinks can be extremely long, and that it is practically impossible to observe such sinks in simulations.

ACKNOWLEDGMENTS

This work was supported in part by the AGH University of Science and Technology, Grant No. 11.11.120.343, and by the Swedish Research Council, Grant No. 2007-523. The first author would like to thank Dr. Bartłomiej Garda for providing access to his computing facilities, where approximately 20% of computations reported in this work have been carried out.

- ¹M. Hénon, *Commun. Math. Phys.* **50**, 69 (1976).
- ²M. Lyubich, *Ann. Math. Second Ser.* **156**, 1 (2002).
- ³M. Benedicks and L. Carleson, *Ann. Math.* **133**, 73 (1991).
- ⁴Z. Galias and W. Tucker, *Chaos* **24**, 013120 (2014).
- ⁵O. Biham and W. Wenzel, *Phys. Rev. Lett.* **63**, 819 (1989).
- ⁶Z. Galias, *Int. J. Bifurcation Chaos* **11**, 2427 (2001).
- ⁷E. Lorenz, *Physica D* **237**, 1689 (2008).
- ⁸D. Sterling, H. R. Dullin, and J. D. Meiss, *Physica D* **134**, 153 (1999).
- ⁹S. Newhouse, *Publ. Math. Inst. Hautes Etudes Sci.* **50**, 101 (1979).
- ¹⁰C. Robinson, *Commun. Math. Phys.* **90**, 433 (1983).
- ¹¹Z. Galias and W. Tucker, *Int. J. Bifurcation Chaos* **23**, 1330025 (2013).
- ¹²P. Grassberger, H. Kantz, and U. Moenig, *J. Phys. A* **22**, 5217 (1989).
- ¹³D. Sterling and J. Meiss, *Phys. Lett. A* **241**, 46 (1998).
- ¹⁴R. Moore, *Interval Analysis* (Prentice Hall, Englewood Cliffs, NJ, 1966).
- ¹⁵A. Neumaier, *Interval Methods for Systems of Equations* (Cambridge University Press, 1990).
- ¹⁶P. Cvitanović, *Physica D* **51**, 138 (1991).
- ¹⁷Z. Galias, *IEEE Circuits Syst. Mag.* **13**, 35 (2013).
- ¹⁸M. Joldes, V. Popescu, and W. Tucker, see <http://hal.archives-ouvertes.fr/hal-00957438> for the technical report.